

Feedforward Control of a Piezoelectric Flexure Stage for AFM

Yang Li and John Bechhoefer

Abstract—We review basic issues in the control of scanning probe microscopes. To improve the performance of the present generation of instruments, we have developed a simple feedforward technique that nonetheless increases the effective bandwidth of the positioning stage by a factor of 15 over its standard operation. If the desired control signal is known in advance (as it is for a periodic scan signal), the feedforward filter can be non-causal: information about the future can be used to cancel the phase lag produced by the stage response. We compare our design with other control techniques. We show that model-based iterative control algorithms can lead to a substantial performance boost, at the cost of more measurements of the system transfer function. We then introduce a model-free variant that is simpler to set up, performs better, and is more robust to system changes.

I. INTRODUCTION

One of the clichés about the development of science is the image of an ever-branching tree, where increasingly specialized domains are viewed as new branches that are connected to each other only by tracing back to the thicker trunks of older growth. Thus, while the disciplines of physics and control engineering share common origins in the study of dynamical systems through the 19th century, their progress in the 20th and 21st centuries has occurred largely in separation from each other. Recently, however, the number of connections between the two disciplines has been increasing notably, as illustrated by two recent reviews by physicists of applications of control theory to physics [1], [2]; by the publication, by control engineers, of the first textbook on modern control theory written for a broad audience of general scientists and engineers [3]; and by the appearance of an interesting “cross-over” work that analyzes physical systems from a control perspective [4].

While influences have gone in both directions, we focus here on applications of control theory to physics. Such applications have come in two forms. First, central concepts of control theory such as positive and negative feedback, feedforward, and robustness have been recognized to be important in the understanding of complex systems, particularly in biological applications [5], [6]. Second, while physicists have for a long time limited themselves to using elementary concepts from control theory, such as PID control, they have recently begun to recognize the value of learning and applying more sophisticated concepts. Such applications have been fruitful in the design of scanning probe microscopes, particularly the atomic force microscope (AFM).

Much of the reason for the interest in applying control concepts to AFM stems from the limitations of simple control algorithms such as proportional-integral (PI) control [7]. The dynamics of the AFM scan head (incorporating both the mechanical resonances of the physical parts and the electro-mechanical response of the piezoelectric actuators) consist of a number of weakly damped poles and of zeros that can be in the right-hand plane (non-minimum phase systems). Controlling such structures is notoriously difficult, and PI algorithms are restricted to low bandwidths [8].

In the present article, we briefly review, in Sec. II, some of the general issues in the control of AFMs. In fact, as both Tien *et al.* [29] and Pao *et al.* [10] have emphasized, the AFM is a MIMO system where the dynamics (and control) of lateral scanners couples to the surface topography sensor, often in significant ways. In this article, we shall simplify by focusing mostly on the dynamics of the lateral scanner. In Sec. III, we present a simple, inversion-based feedforward control algorithm for AFM scanners. In Sec. IV-A, we compare our method to a previously derived iterative method. In Sec. IV-B, we introduce a “model-free” variant with significant advantages.

II. REVIEW OF CONTROL ISSUES RELATING TO AFM SCANNERS

Most current commercial AFMs are slow, with high-quality images typically taking several minutes. Such slow speeds can be traced back to the resonant frequencies of the scanner (≈ 0.1 – 1 kHz) and the bandwidth of the combination of cantilever sensor, vertical mechanical scanner, and control system used to measure sample topography (≈ 1 kHz) – “sensor,” for short. (The sensor bandwidth must exceed the line-scan frequency by a factor equal to the number of pixels, typically 100 to 1000 in each direction.) Higher-speed AFM imaging is desirable, both because many applications require imaging of fast processes and for operator comfort and efficiency [11]. For example, to achieve “video” rates of 25 images/s at 200 pixels square implies scanner bandwidths of at least 10 kHz (for a sinusoidal scan) and sensor bandwidths of at least 2 MHz. For closed-loop operation and constant-velocity scans, these bandwidths would need to be multiplied at least ten-fold. Such bandwidths are being approached in recent instruments [12], [13], [14], [15].

It is useful to consider what sets the bandwidth in current AFMs. Since the control algorithms are scaled by the characteristic frequencies (i.e., resonances), the bandwidth is determined both by the physical resonance frequencies and the ability of the control algorithm to perform well at frequencies close to the resonances. While the focus here

This work was supported by NSERC (Canada).
Dept. of Physics, Simon Fraser University, Burnaby, BC, V5A 1S6,
Canada. E-mail: johnnb@sfu.ca.

is on the control aspects, we briefly review the physical limitations. (See [16] for a more in-depth discussion.)

The physical frequency limits of AFM are associated with the mechanical resonances of the lateral scanner, the vertical scanner, and the cantilever sensor. Most commercial AFMs have scanner dimensions of order cm and cantilever-tip assemblies with lengths of order 100 μm , with scanner resonances of order 100–1000 Hz and cantilever resonances of order 10–100 kHz. Resonance frequencies ν are set by the size and shape of objects: $\nu \sim c/(\ell a)$, with c the sound speed, ℓ the largest dimension, and a the aspect ratio (ratio of largest length to smallest) [17]. Putting $c \approx 10^3$ m/s, $\ell \approx 1$ cm, and $a \approx 10$ gives ≈ 100 Hz for the scanner; with $\ell \approx 100$ μm and $a \approx 100$ (typical for a commercial cantilever), we get ≈ 100 kHz. One might naively think that the aspect ratio should be 1 (cube-like structures), in order to maximize the resonance frequency. But other factors favor large aspect ratios. There is a maximum electric field that piezoelectric materials can withstand, which leads to a maximum displacement. The practical way to increase the scan range is to put piezo elements in series, increasing the aspect ratio. For cantilevers, larger aspect ratios make softer probes, which minimize sample damage. The key, then, to increasing the lowest resonance frequencies of both scanner and cantilever is to use smaller overall length scales and, as far as possible, lower aspect ratios. An interesting new scanner design uses conventional parts and machining but reduces ℓ and a to achieve resonances of 22 and 40 kHz (lateral and vertical directions) [18]. In parallel, smaller cantilevers have been explored for a number of years [19] and are beginning to be produced commercially [11]. The ultimate solution would be to scale the entire AFM down to a microfabricated chip [20].

Scaling down both scanner and tip sizes is only part of the solution, however. In a typical commercial AFM, scan speeds are limited to a few Hz, even though the scanner resonances are a few hundred Hz. The ratio of the scanning bandwidth to physical scanner resonance is thus only ≈ 0.01 . The feedforward technique to be presented here allows one to increase this ratio easily to 0.1 and, with more effort, to 0.3. Our technique [22], is only one of a number of advanced control techniques for AFM that have been discussed recently (reviewed in [10]), and we place our scheme in the context of others, below.

III. A SIMPLE IMPLEMENTATION OF INVERSION-BASED FEEDFORWARD CONTROL OF AN AFM SCANNER STAGE

In this section, we outline a simple, practical version of feedforward to improve the scan rates of a commercial piezoelectric flexure stage [21]. The design is an improved version of one we presented recently [22]. The basic idea of feedforward is to use the known dynamical characteristics of a system to design a prefilter that “inverts” those dynamics as far as possible, so that the output more closely resembles the desired input. Our goal was to achieve reasonable performance while keeping the design as simple as possible. Simplicity has two virtues: first, the design is compatible with

many existing commercial AFMs; second, the design can be understood and implemented by users without extensive control-theory background. This latter reason was important, as a secondary goal of our work was to proselytize the virtues of using feedforward to the physics community, where it has been seldom applied.

In our work, we implemented feedforward on a closed-loop piezoelectric flexure stage [21]. Such stages are becoming more standard on commercial instruments and have two advantages over the tube scanners of older AFMs: first, they incorporate position sensors that allow the internal feedback of the stage to compensate, at low-frequencies, for the hysteresis and creep found in the open-loop response of piezoelectric elements. Although there have been attempts to invert the nonlinear, hysteretic models that describe the piezo-actuator response, the models are difficult and require extensive characterization of the scan response under different conditions. Correcting as much of that motion in feedback makes the feedforward task much easier [23]. A second advantage of using a commercial flexure stage is that the flexure mechanisms do a better job of decoupling dynamics, particularly horizontal-vertical coupling [29].

Since the feedback in the translation stage is effective at low frequencies in linearizing the stage response, we can describe that response by a linear transfer function, $T(s)$, which represents the closed loop dynamics. Fig. 1 shows the measured response of our stage. The two-pole, low-pass filter part of the dynamics, with a bandwidth of 27 Hz, arises from the feedback electronics of the stage. We see here the origin of the small ratio of practical scanning rates (scan lines/time) to resonance frequency. Because of the lightly damped mechanical stage resonance at ≈ 440 Hz, it would be difficult to set the closed-loop bandwidth higher. Without feedforward, scans should be at no more than 10% of the feedback bandwidth, in order to prevent attenuation and lag of the higher harmonics of the triangle-wave scan signal. Thus, one arrives at scan rates of 2-3 lines/sec., which is typically the maximum used in AFMs based on such scanners.

The feedforward design presented in [22] approximates the inverse of the response shown in Fig. 1. It is important to realize that an exact inverse, which would trivially lead to exact tracking of the output by the input, is never possible. First, the transfer function is never perfectly known. Second, all stable poles become zeroes in the inverse. This means that they are approximately differentiators and require a frequency response that increases indefinitely at high frequencies. For example, a simple pole, $1/(1+s)$, becomes a simple zero, $1+s$, whose magnitude response increases linearly with frequency at high frequencies. Such a response cannot be exactly realized by any physical actuator, whose response will always roll off at high-enough frequencies. Third, if the system is non-minimum phase, then the inverse has unstable poles. Devasia *et al.* have come up with clever ways to deal with this situation, albeit at the cost of using a non-causal prefilter [24]. Here, one of the benefits of using a closed-loop translation stage is that its dynamics are well-

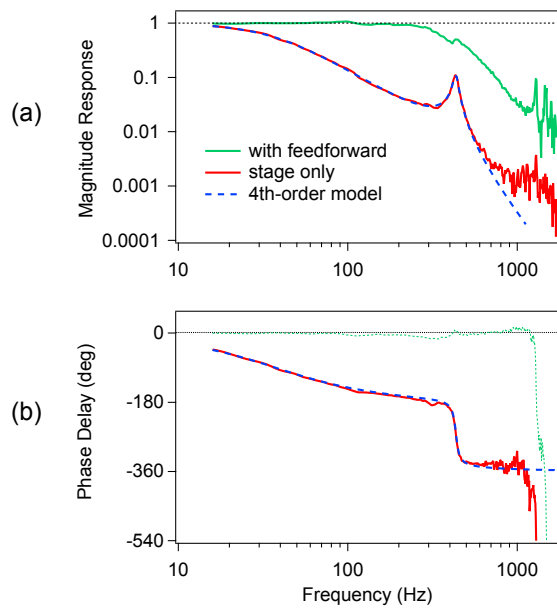


Fig. 1. Magnitude (a) and phase (b) Bode plot of translation stage response. Dashed curves are fit to a fourth-order model. The response after compensation by the pre-filter is also shown.

described by a minimum-phase transfer function at relevant frequencies (Fig. 1).

In our work, we arrive at a physically realizable response by shifting the poles of the response function to higher frequencies. These are kept below the first mechanical resonance but may be much closer than the closed-loop bandwidth. In the case considered here, the chosen bandwidth was 400 Hz, which nearly equals the lowest mechanical resonance of the stage, 430 Hz. We then constructed our approximation to the transfer-function inverse by placing zeros on top of each pole (covering the feedback poles and the first mechanical resonance). Having put four zeroes in our pre-filter (two for the feedback loop and two for the mechanical resonance), we added four poles, in order to keep the prefilter response finite at high frequencies. The poles corresponding to the feedback were placed in a Butterworth configuration giving the desired increased bandwidth (400 Hz). The Butterworth configuration gives the flattest amplitude response. The poles corresponding to the mechanical resonance were left at the resonance frequency, but the damping of that resonance was shifted to be at critical damping. The continuous-time transfer function was converted into a discrete-time version using the Tustin (bilinear) transform [25], with a sampling rate of 10 kHz. Our filter is implemented as an infinite-impulse-response (IIR) filter, which requires fewer coefficients than the alternative, finite-impulse-response (FIR) filters championed by Seering and collaborators [26]. The IIR filter is of the form,

$$r'_n = a_2 r_n + a_1 r_{n-1} + a_0 r_{n-2} - b_1 r'_{n-1} - b_0 r'_{n-2}, \quad (1)$$

with r the desired input and r' the modified input, and where the a and b coefficients are taken from the discrete-time

version of the pre-filter. Fig. 2 shows traces illustrating the improvement for various scan speeds.

One limitation of using a feedforward pre-filter on a closed-loop positioning stage is that the finite bandwidth of the closed-loop controller (the low-pass response in Fig. 1) limits the bandwidth obtainable by the pre-filter. In essence, the modified input must be amplified at high frequencies. At frequencies that are too high, the amplification factor can easily cause the desired stage input signal to be clipped by its finite input range. One can, of course, restrict the range and work in the central part of the overall scanner range. But there will always be a practical limit. In our case, with a bandwidth of 400 Hz., we could perform scans of 10 μm at 150 Hz before being limited by the range of the piezo actuator.

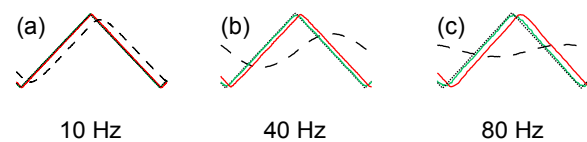


Fig. 2. Measured stage responses at (a) 10 Hz, (b) 40 Hz, and (c) 80 Hz. Dotted-line triangular waveform represents the desired stage response (1 μm amplitude). Dashed line shows the phase shifted and attenuated stage response without feedforward. Red lines show the response with a causal feed-forward filter giving 400 Hz system bandwidth. Green lines show the response with a similar non-causal filter.

One advantage of using a feedforward pre-filter is that the repetitive nature of the desired triangle-wave scan allows one to design a non-causal prefilter. Intuitively, with future knowledge of the signal, one can send a control input to the stage in advance of the desired movement, such that the phase advance of each frequency component just cancels out the delay due to the stage inertia. A simple way to compute the desired waveform is sketched in Fig. 3, with the results for the scan signal illustrated in Fig. 2. The basic idea is to first pass the signal through the pre-filter and a model of the system's dynamics. This generates a conventional, phase-delayed signal. That signal is then time reversed and passed again through the pre-filter. All these steps are done computationally. Finally the signal is passed through the physical stage. The combined dynamics of pre-filter and stage then remove the phase delays generated in the first pass, resulting in a signal with zero-phase shift. In Fig. 2, one can see clearly that the non-causal filter removes nearly all phase shift relative to the reference. The small residual shift noticeable at 80 Hz is due to the unmodeled dynamics that begin to be important at 1 kHz.

In principle, in order to implement a non-causal filter exactly, one should know the desired input signal out to infinite times in the future. In practice, because the stage dynamics decay, knowledge of the future to a specified accuracy is required only to finite times. Zou and Devasia have used this idea to develop a more sophisticated approach, where a finite-time "preview" is all that is needed [27]. In the case of AFM images, such an approach is typically not needed, in that the scanning waveform is periodic, except

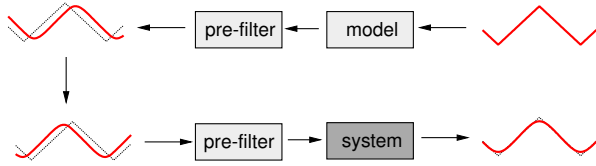


Fig. 3. Sketch of a non-causal feedforward filter. The light-shaded boxes represent modeled dynamics, while the dark-shaded box represents the physical system.

at the beginning and end of scanning. We thus generate the required input waveform by inputting a waveform with several (usually five) periods and then carrying out the rest of the procedure illustrated in Fig. 3 with the steady-state response. This gives a signal appropriate for a perfectly periodic signal but which generates errors in the transient when the first scan starts from rest. But simply adding a scan line before starting the image proper easily removes any effects of transient scanner dynamics. (Note here that “transient” refers to the motion that occurs when the scanner starts from rest and not to the motion occurring when the stage reverses direction. The latter is corrected by the non-causal filter.)

IV. ITERATIVE METHODS

The inversion-based design presented above is deliberately simple and complements the more sophisticated techniques presented within the control community. For example, a variant of optimal control tries to compensate for the uncertainties in the dynamics by using notions of robust control (\mathcal{H}^∞ metric) for the cost function [7], [28]. In another approach, Tien, Zou, and Devasia [29] have explored feedforward techniques where they supplement the kind of inversion-based techniques discussed here with a procedure inspired by iterative learning control schemes [30], [31], [32]. The basic idea is to apply a control repeatedly to a system, to measure the outcome, and to use the difference between observed and desired outcome to improve the control signal. As Tien *et al.* note, such a scheme applies well to many AFM operations, such as XY-stage scanning, where the control signal is already periodic. They further note that the periodicity makes it natural to formulate the iterative method in frequency space. Here, we summarize the iterative approach, implement it on our AFM stage, and compare its performance to the simple inversion-based design discussed above. We then go on to introduce a significant variation of our own, which eliminates the preliminary modeling step.

A. Model-based iterative control

Here, we describe a variant of the iteration method introduced by Kim, Zou, and Su [33]. Because estimates of the system transfer function (and related uncertainties) play a key role in the algorithm, we refer to their method as “model based.” Let the actual system transfer function be denoted by $G^*(j\omega)$ and the experimentally determined model by $G(j\omega)$.

Then one starts with a control signal that, in the frequency domain, is given by

$$u_0(j\omega) = G^{-1}(j\omega) y_d(j\omega), \quad (2)$$

where $y_d(j\omega)$ is a frequency component of the desired sensor signal, $y_d(t)$. Here, one takes advantage of the fact that a repetitive control process is naturally analyzed in the frequency domain. One measures N periods of the repetitive waveform, Fourier transforms, calculates the update for each Fourier component, and transforms the result back to the time domain to find the desired control signal, $u(t)$. After applying the initial control signal, one measures the actual output $y(j\omega)$ and updates the control signal as

$$\begin{aligned} |u_k| &= |u_{k-1}| + \rho G^{-1}(|y_d| - |y_{k-1}|), \quad k \geq 1, \quad (3) \\ \angle u_k &= \angle u_{k-1} + (\angle y_d - \angle y_{k-1}). \end{aligned}$$

In Eq. 3, all quantities are functions of $j\omega$. Kim *et al.* show that the iteration law in Eq. 3 is stable provided that the free parameter ρ is chosen to be in the range $0 < \rho < 2/\Delta G$, where $\Delta G = G^*/G$ is a measure of the uncertainty in the determination of the transfer function at the given frequency ω . One cannot directly measure ΔG since G^* is unknowable, but it may be estimated by the spread of repeated measurements of the transfer function. Specifically, we inject white noise for the transfer-function measurements and take the ratio of the maximum to minimum values over 10 runs, sampling at 10 kHz for 1 s. Below 500 Hz, $\Delta G < 1.2$, increasing to 2 by 1 kHz. Above that frequency, we truncate all harmonics in u .

Using the measured G (Fig. 1) and setting $\rho = 1/\Delta G$, we obtain the measured 80 Hz waveforms and residuals shown in Fig. 4(b) and (e). Comparing to the results obtained with the inversion-based feedforward method (a) and (d), we see a noticeable improvement, which we ascribe to two factors: first, the slight phase shift due to modeling errors in the inversion-based method is removed. Second, the bandwidth of the iterative method was 1 kHz, in contrast to the 400 Hz bandwidth of the inversion-based method. Indeed, one notes that an advantage of the iterative method is that it is not limited by any particular bandwidth per se; rather, what counts is how accurate the transfer-function measurement is at any particular frequency. When $\Delta G \gg 1$, ρ will be very small, and the combination of sensor and actuator noise will prevent any meaningful convergence of u to its optimal value. But this condition is independent of where mechanical resonances lie. Of course, in general uncertainties will be greatest near resonances, since they can be narrow in piezoscanners and shift around in frequency as a function of changing mechanical load, etc.

We also compared the driving wave forms for the methods. Fig. 5(a) shows the non-causal inversion-based driving signal (solid line). We note how it starts to alter the motion before the output wave form reverses (dotted line). Fig. 5(b) shows the same signals for the model-based iterative scheme. The large-amplitude, high-harmonic at 800 Hz does not appear in the inversion-based input signal, as it is beyond the

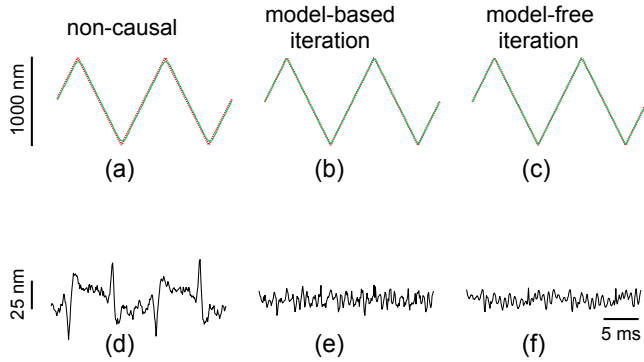


Fig. 4. Waveforms and residual tracking errors for three different control algorithms. (a) Inversion-based feedforward; (b) Model-based iteration; (c) Model-free iteration. Measured sensor signal (green) is nearly perfectly superposed on the tracking signal (red) in all three cases. (d-f) Residual tracking errors for the respective control algorithms. 80 Hz, 1 μm peak-to-peak amplitude.

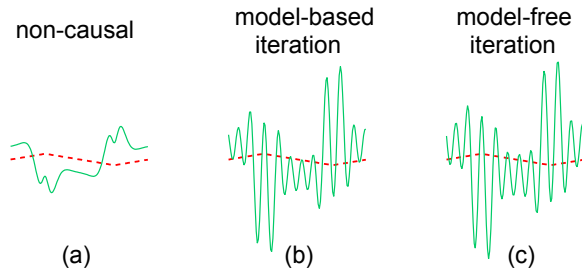


Fig. 5. Driving wave forms. (a) Causal inverse. (b) Non-causal inverse. (c) Model-based iteration; (d) Model-free iteration. Dashed red line is the measured sensor signal; solid green line is the actuator signal sent to the stage. 80 Hz, 1 μm peak-to-peak amplitude.

bandwidth of that controller. Its large amplitude here may be mostly traced back to the low-pass filter in the analog feedback loop of the piezo stage.

B. Model-free iterative control

While the model-based iterative control improves the tracking error noticeably, it is at the cost of additional complexity. One must first measure the transfer function repeatedly, ideally under a wide range of circumstances (including variations in driving amplitude and offset, stage load, etc.) in order to estimate the uncertainties ΔG . Second, the actual iteration scheme must be implemented. The second concern is a one-time effort; the first is more worrisome in the sense that entire set of possible experiments and their consequential variations in G must be anticipated.

In order to circumvent these issues, we introduce a model-free variation of the method of Kim *et al.*.

- 1) We use the most recent input-output measurement to estimate $G^{-1} \approx u_{k-1}/y_{k-1}$.
- 2) We choose $\rho = 1/\Delta G$, the value that converges most rapidly for linear, noiseless dynamics. (For weak nonlinearity and noise, we do not anticipate that the optimal value will shift greatly.)

3) We acquire data over a block of N periods to reduce sensor and actuator noise.

4) We initialize with the naive transfer function, $G = 1$.

Putting all of this together, we arrive at the following control algorithm:

$$\begin{aligned} u_0 &= y_d, \\ |u_k| &= |u_{k-1}| \frac{|y_d|}{|y_{k-1}|}, \quad k \geq 1, \\ \angle u_k &= \angle u_{k-1} + (\angle y_d - \angle y_{k-1}). \end{aligned} \quad (4)$$

While we have not investigated the theoretical convergence properties of the model-free algorithm presented here, we have observed that it performs slightly better than the model-based iterative algorithm. In Fig. 4, parts (c) and (f) show the sensor signal and residuals for our new algorithm. Both waveforms look “perfect” at the scale drawn, while the residuals for the model-free algorithm are slightly lower. In Table I, we show the rms and sup-norm error for all three methods. The model-free method has the lowest error level, presumably because it eventually develops a model estimate that is better than the one we used for the model-based method. Both methods are substantially better than the non-causal feedforward method presented above. The main reason for the higher error comes from poorer tracking of the corners (where the stage reverses its velocity). This is to be expected, since its bandwidth was lower (0.4 vs. 1 kHz).

TABLE I

STEADY-STATE ERRORS FOR THE DIFFERENT CONTROL ALGORITHMS. 80 HZ, 1 μM PEAK-TO-PEAK AMPLITUDE, 100 PERIODS/ITERATION, AVERAGED OVER 15 ITERATIONS AFTER AN INITIAL TRANSIENT OF 15 ITERATIONS.

	$E_2(\%)$	$E_\infty(\%)$
non-causal	8.3	11.1
model-based	1.8	4.4
model-free	1.2	3.5
sensor & actuator noise	0.7	2.0

In Fig. 6, we show the iteration dependence of the rms errors. The model-free algorithm was based on measuring 1 period/iteration, while the model-based algorithm was given 10 periods/iteration. (If we used only one period, it did not converge.) As expected, the model-based algorithm initially had a lower error, as its initial guess was based on previous measurements of the transfer function while the model-free algorithm takes y_d as its initial guess. Still, after 5 iterations, the model-free algorithm converged to an error level slightly below that of the model-based algorithm.

We then tested the robustness of both algorithms. At iteration 8, we added a mass of 200 gm, which lowered the resonance from 440 to 400 Hz (10%). The model-free algorithm recovered again in 3 iterations, while the model-based algorithm recovered noticeably more slowly. This is also to be expected: the model-based algorithm mis-estimates the uncertainties of the now-altered transfer function. At

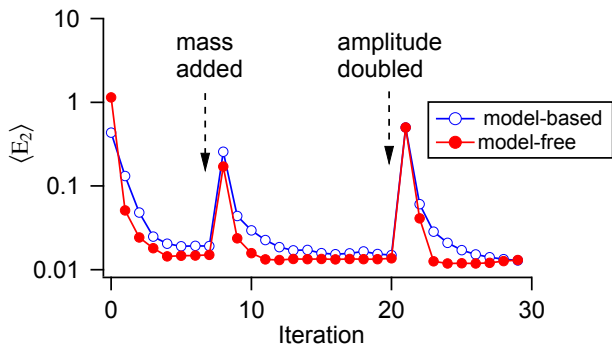


Fig. 6. Tracking errors in the model-based and model-free iteration algorithms. Control-signal updates are calculated using one period for the model-free and ten periods for the model-based algorithms. Initial transient error of the model-free algorithm converges to steady state after 3 iterations. First arrow shows effects of adding a 200 gm mass to stage; second arrow shows effects of doubling output amplitude to $2 \mu\text{m}$. Waveform of 80 Hz.

iteration 21, we doubled the amplitude of the driving signal. Again, the model-free algorithm recovered rapidly, while the model-based algorithm was slower.

We also measured the effects of sensor and actuator noise and found that each contributed about 0.35% rms relative to the amplitude of driving wave form that we used. This implies that systematic errors, most likely due to nonlinear effects, account for the rest of the errors.

V. DISCUSSION

The motivation for introducing our inverse-based feedforward prefilter and applying it to a closed-loop scanning stage was to combine the simplicity of working with a closed-loop scanner with the larger bandwidths made possible by the use of the approximate inverse to the closed-loop transfer function. Using a closed-loop stage helps circumvent the delicate issues involved in modeling piezoelements [23]. We found that a relatively simple transfer-function measurement could be used to increase the effective bandwidth of the stage by a factor of roughly 15, reaching nearly its main mechanical resonance frequency. The inversion-based feedforward filter is straightforward to set up and implement.

One issue with the inversion-based feedforward technique is its lack of robustness. The inversion is helpful only to the extent the transfer function is known accurately. Devasia has addressed this issue [34] and found that the optimal level of feedforward depends inversely on the uncertainty in the system's dynamics, for linear systems in the frequency domain. The conclusion is that one should limit feedforward to those frequencies where the dynamics are well known. In the work presented above, the feedforward does this by using a low-pass filter to turn off its effects for frequencies that exceed the maximum used in the transfer-function model.

The iterative schemes that we addressed in the second part of the paper take a fundamentally different approach, in that one uses the measured output signal to reshape the input signal, forcing a convergence of the actual output to that desired. In the formulations of Devasia, Zou, and collaborators, this

iteration is done offline and the result is implemented as a feedforward filter. In the model-free variant presented here, it is natural to implement the iteration continuously online. In modern AFMs, one usually acquires the sensor signal from the scanning stage anyway. The additional computational effort to perform the forward and reverse Fourier transforms is negligible, especially considering that one need update only every scan periods. (Actually, for noise reduction and better frequency resolution, one might well want to measure – and hence update – in blocks of several periods.) Further, modern AFM controllers use DSP and FPGA processors that can easily run a variety of real-time processes in parallel. In the work presented here, the iterations are done continuously on an AFM scanner stage, but the software has yet to be integrated with the rest of the AFM control program.

By performing the iterative scheme online, one gains all the advantages of robustness illustrated above in Fig. 6. Even for large changes in the driving signal or in the transfer function, the iteration leads to a rapid recovery. The robustness to changes in the transfer function are striking in that they would render the inverse-based feedforward scheme useless. Each mechanical resonance is “zeroed out,” and a large change in the transfer function would require further offline measurements. In the iterative scheme, they are handled automatically, with no outside intervention. In effect, the robustness here is reminiscent of that associated with ordinary feedback. Here, the difference is that the feedback is over slow time scales (several periods of the driving frequency) and is thus easy to implement.

One challenge for the iterative control scheme is that the higher bandwidths, which are an important factor in the tracking improvements, require larger amplitudes for the driving waveform. We can trace that back to the combination of the closed-loop control, with its low-pass filter, and the fact that we include frequencies above the principal mechanical resonance of the system. Bypassing the stage's feedback loop and applying the control signal directly to the piezos will partly resolve the problem by making the system response roll off more slowly at high frequencies. Of course, one then loses the advantages of having a feedback controller eliminate the nonlinearities, hysteresis, creep, etc. of the stage. These problems will be at least partially offset by the iterative nature of the control algorithm.

Other issues with model-free iterative control that need to be worked out include the effect of nonlinearities and methods for correcting external disturbances.

VI. CONCLUSION

We have presented a simple, practical feedforward design that significantly improves the performance of commercial piezoelectric translation stages used in atomic force microscopy and other applications of nanoscience. Increasing the overall speed of AFM measurements requires revamping many aspects, including both hardware and software, and the work presented here is just one part of such an effort.

We then examined an alternate control based on iterative learning algorithms. We showed that the model-based algo-

rithm of Devasia, Zou, and collaborators could substantially improve the performance, at the cost of additional measurements and programming. We then introduced a model-free variant of the iterative control method that slightly exceeded the model-based algorithm in performance but was easier to implement (no model to measure, no parameters to tune) and more robust to changes in the system transfer function. This method merits further study.

We began this contribution by noting the common view of the development of science as a growing, ever-branching tree. In this contribution, we have given an example of new connections made between two branches that split away from each other many years ago. Such “reconnections” have become increasingly popular in many parts of science in the guise of “interdisciplinary research,” where it is recognized that progress on difficult problems requires contributions from a variety of disciplines. Perhaps a more appropriate image of the development of science might be that of a complex, growing network, with numerous and unexpected connections between different domains.

VII. ACKNOWLEDGMENTS

We gratefully acknowledge support from NSERC (Canada). JB also thanks Lucy Pao, Qingze Zou, and the other organizers of the AFM sessions of ACC 2008 for encouraging cross-disciplinary dialog. We thank especially the anonymous referee who suggested we compare our inverse-based feedforward scheme to others.

REFERENCES

- [1] J. Bechhoefer, “Feedback for Physicists: A Tutorial Essay on Control,” *Rev. Mod. Phys.*, vol. 77, 2005, pp. 783–836.
- [2] M. Schulz, *Control Theory in Physics and other Fields of Science: Concepts, Tools and Applications*, Springer-Verlag, Berlin; 2006.
- [3] K.J. Åström and R.M. Murray, *Feedback Systems: An Introduction for Scientists and Engineers*, Princeton University Press, Princeton, NJ; 2008.
- [4] A.L. Fradkov, *Cybernetical Physics*, Springer-Verlag, Berlin; 2007.
- [5] E.D. Sontag, “Molecular Systems Biology and Control,” *Euro. J. Control*, vol. 11, 2005, pp. 396–435.
- [6] U. Alon, *An Introduction to Systems Biology : Design Principles of Biological Circuits*, Chapman & Hall/CRC Press, Boca Raton, FL; 2007.
- [7] S. Salapaka, A. Sebastian, J.P. Cleveland, M.V. Salapaka, “High Bandwidth Nano-Positioner: A Robust Control Approach,” *Rev. Sci. Instr.*, vol. 73, 2002, pp. 3232–3241.
- [8] S. Skogestad and I. Postlethwaite, *Multivariable Feedback Control: Analysis and Design.*, 2nd ed., Wiley, New York, 2005.
- [9] S. Tien, Q. Zou, and S. Devasia, “Iterative Control of Dynamics-Coupling-Caused Errors in Piezoscanners during High-Speed AFM Operation,” *IEEE Trans. Cont. Sys. Tech.*, vol. 13, 2005, pp. 921–931.
- [10] L.Y. Pao, J.A. Butterworth, and D.Y. Abramovitch, “Combined Feedforward/Feedback Control of Atomic Force Microscopes,” in *Proc. Am. Control Conf.*, New York, NY, 2007, pp. 3509–3515.
- [11] P.K. Hansma, G. Schitter, G. E. Fantner, and C. Prater, “High-Speed Atomic Force Microscopy,” *Science*, vol. 314, 2006, pp. 601–602.
- [12] T. Ando, N. Kodera, E. Takai, D. Maruyama, K. Saito, and A. Toda, “A High-Speed Atomic Force Microscope for Studying Biological Molecules,” *Proc. Nat. Acad. Sci. (USA)*, vol. 98, 2001, pp. 12468–12472.
- [13] A.D.L. Humphris, M.J. Miles, and J.K. Hobbs, “A Mechanical Microscope: High-Speed Atomic Force Microscopy,” *Appl. Phys. Lett.*, vol. 86, 2005, No. 032106.
- [14] M.J. Rost, L. Crama, P. Schakel, E. van Tol, G.B.E.M. van Velzen-Williams, C.F. Overgaw, H. ter Host, H. Dekker, B. Okhuijsen, M. Seynen, A. Vijftigschild, P. Han, A.J. Katan, K. Schoots, R. Schumm, W. van Loo, T.H. Oosterkamp, and J.W.N. Frenken, “Scanning Probe Microscopes Go Video Rate and Beyond,” *Rev. Sci. Instr.*, vol. 76, 2005, No. 053710.
- [15] G.E. Fantner, G. Schitter, J.H. Kindt, T. Ivanov, K. Ivanova, R. Patel, N. Holten-Andersen, J. Adams, P.J. Thurner, I.W. Rangelow, and P.K. Hansma, “Components for High Speed Atomic Force Microscopy,” *Ultramicroscopy*, vol. 106, 2006, pp. 881–887.
- [16] G. Schitter, “Advanced Mechanical Design and Control Methods for Atomic Force Microscopy in Real-Time,” *Proc. Am. Contr. Conf.*, New York, NY, 2007, pp. 3503–3508.
- [17] D. Sarid, *Scanning Force Microscopy: Applications to Electric, Magnetic, and Atomic Forces*, Oxford Univ. Press, New York; 1991, Sec. 1.9.
- [18] G. Schitter, K.J. Åström, B. DeMartini, G.E. Fantner, K. Turner, P.J. Thurner, and P.K. Hansma, “Design and Modeling of a High-Speed Scanner for Atomic Force Microscopy,” *Proc. Am. Contr. Conf.*, Minneapolis, MN, 2006, pp. 502–507.
- [19] D.A. Walters, J.P. Cleveland, N.H. Thomson, P.K. Hansma, M.A. Wendman, G. Gurley, and V. Elings, “Short Cantilevers for Atomic Force Microscopy,” *Rev. Sci. Instr.*, vol. 67, 1996, 3583–3590.
- [20] S. Hafizovic, D. Barrettino, T. Volden, J. Sedivy, K.-U. Kirstein, O. Brand, and A. Hierlemann, “Single-Chip Mechatronic Microsystem for Surface Imaging and Force Response Studies,” *Proc. Nat. Acad. Sci.*, vol. 101, 2004, pp. 17100–17015.
- [21] Mad City Labs, Madison, WI. Model Nano-H100.
- [22] Y. Li and J. Bechhoefer, “Feedforward Control of a Closed-Loop Piezoelectric Translation Stage for Atomic Force Microscopy,” *Rev. Sci. Instr.*, vol. 78, 2007, no. 013702.
- [23] D. Croft, G. Shed, and S. Devasia, “Creep, Hysteresis, and Vibration Compensation for Piezoactuators: Atomic Force Microscopy Application,” *J. Dyn. Sys., Meas., and Control*, vol. 123, 2001, pp. 35–43.
- [24] S. Devasia, D. Chen, and B. Paden, “Nonlinear Inversion-Based Output Tracking,” *IEEE Trans. Aut. Cont.*, vol. 41, 1996, pp. 930–942.
- [25] G.F. Franklin, J.D. Powell, and M. Workman, *Digital Control of Dynamic Systems*, 3rd. ed., Addison Wesley, Menlo Park, CA, 1998.
- [26] The group at MIT led by W. P. Seering has been a particular champion of feedforward (or “input shaping”) techniques. For a detailed and lucid introduction, see W. E. Singhose, Ph. D. Thesis, MIT (1997).
- [27] Q. Zou and S. Devasia, “Preview-Based Optimal Inversion for Output Tracking: Application to Scanning Tunneling Microscopy,” *IEEE Cont. Sys. Tech.*, vol. 12, 2004, pp. 375–386.
- [28] G. Schitter, F. Allgöwer, and A. Stemmer, “A New Control Strategy for High-Speed Atomic Force Microscopy,” *Nanotech.*, vol. 15, 2004, pp. 108–114.
- [29] S. Tien, Q. Zou, and S. Devasia, “Iterative Control of Dynamics-Coupling-Caused Errors in Piezoscanners During High-Speed AFM Operation,” *IEEE Trans. Cont. Sys. Tech.*, vol. 13, 2005, pp. 921–931.
- [30] S. Arimoto, S. Kawamura, and F. Miyazaki, “Bettering Operation of Dynamical Systems by Learning: A New Control Theory for Servomechanism or Mechatronics Systems,” *Proc. of 23rd Conf. on Decision and Control*, 2003, pp. 1064–1069.
- [31] J.J. Craig, “Adaptive Control of Manipulators through Repeated Trials,” *Proc. Am. Contr. Conf.*, San Diego, CA, 1984, pp. 1566–1573.
- [32] J. Ghosh and B. Paden, “Iterative Learning Control for Nonlinear Non-minimum Phase Plants,” *J. Dyn. Sys., Meas., and Control*, vol. 123, 2001, pp. 21–30.
- [33] K.-S. Kim, Q. Zou, and C. Su, “Iteration-based Scan-Trajectory Design and Control with Output-Oscillation Minimization: Atomic Force Microscope Example,” *Proc. Am. Contr. Conf.*, New York, NY, 2007, pp. 4227–4233.
- [34] S. Devasia, “Should Model-Based Inverse Inputs Be Used as Feedforward Under Plant Uncertainty?” *IEEE Trans. Aut.Cont.*, Vol. 47, 2002, pp. 1865–1871.